MSEC2020-8258

SEMICONDUCTOR ASPECTS
OF THE OXYFUEL CUTTING TORCH PREHEAT FLAME

PART I: MEASUREMENTS BETWEEN TORCH AND WORK

Christopher R. Martin[*]
Teresa Pond
Jacob Tomas
Jenna Schmit
Erikson Miguel
Altoona College
Penn State Unviersity
Altoona, PA

Alex Untaroiu
Kemu Xu
Department of Mechanical Engineering
Virginia Tech
Blacksburg, VA

ABSTRACT

This two-part paper presents precise measurements of the ion currents passing between the torch and work piece of the preheat flame of an oxyfuel cutting torch as a means for replacing contemporary sensing suites. Part I shows that the current-voltage characteristic of the flame exhibits sharp discontinuities common to semi-conductors that we study in various configurations including preheat, pierce, cut, and loss-of-cut. Standoff measurements are made by applying a sinusoidal current signal between the torch and work piece while the resulting voltage amplitude is an indication of flame resistance. Uncertainties are estimated to range from 0.5mm to 1mm (.02in to .04in). Signals for ready-to-pierce and precursors for loss-of-cut are also produced due to the generation of secondary ions from chemical activity at the work piece.

1 Introduction

Investigations into the electrical behaviors of the oxyfuel preheat flame have been encouraged by persistent challenges fully automating this century-old process with excellent cutting performance on thick steels. By burning away steel in a pure oxygen jet, the properly tuned oxyfuel torch benefits from heat release along the full depth of the kerf, but the process has proven especially harsh on the sensors that are necessary for automation.

Consider, for example, methods to measure the distance between the torch tip and the work piece. Radiative and abrasive particulates plague optical measurements. Dependencies on temperature, humidity, relative location to the plate edge, and proximity to other torches frustrate popular magnetic and capacitive methods. Mechanical contact methods like plate riders rarely live long and suffer from irregularities in the work surface. In fact, all of these methods suffer from limited sensor life with serious implications on the reliability of the process.

It is important to emphasize that that the standoff distance is only one of many parameters that must be monitored to ensure the quality of the cutting process. Despite receiving more attention than any other attribute of the process, contemporary standoff sensors still leave room for improvement. Meanwhile, other process parameters are even less reliable when sensed at all: e.g. ready-to-pierce, loss-of-cut, flameout, edge-of-plate.

1.1 Ion Currents

Electrical currents in most flames are due to motions of ionized hydronium molecules (H_3O^+) and their liberated electrons. They are intermediate species in a complex series of reactions that were not identified until the second half of the twentieth

[*]Email: crm28@psu.edu

century [1, 2, 3]. This chemical means for forming a plasma distinguishes these "chemions" from their "collisionally" generated counterparts in arcs and thermal plasmas. Perhaps the most striking difference is the severe disparity in charge carrier mass; about 33,000:1 for H_3O^+ and the free electron, but only about 1,800:1 for thermally ionized hydrogen. These advances are well reviewed by Fialkov [4].

The semiconductor behavior in flames is due to the limited supply and dissimilar mobility of the charge carriers. By applying even weak electric fields in atmospheric flames, free electrons can be made to drift, leaving the slower positively charged molecules in their wake. When the field is so strong that electrons have completely evacuated a region adjacent to a negative metal surface, the current to the surface will be entirely determined by the concentration of the remaining nearby positive ions. When this occurs, additional field strength makes only a weak impact on the current, and the current is said to be "saturated;" a semi-conductor characteristic.

1.2 The Oxyfuel Preheat Flame

A US patent issued to Mott, Chouinard, and Harding in 1944 may be the earliest public record of a proposal to use the electrical properties of the preheat flame as a sensor [5]. At that time, it was well established that flames can be made to conduct electricity, it was known that flames could be driven to saturation in ways we now associate with semiconductors [6, 7]. In the time since, the patent record shows continued work on ion current sensing in oxyfuel flames [8, 9, 10, 11, 12], but with no record of a prototype available for critical scrutiny. Meanwhile, significant work has been done to apply ion current sensing in propulsion systems [13, 14], to internal combustion engines [15, 16, 17, 18], and (with great success) to furnaces [19, 20, 21].

Despite the amount that has been learned about ion currents in recent decades, and despite the parallel advances in other industries, there seems to be no record of fundamental studies into the electrical properties of the oxyfuel preheat flame prior to works published by the authors in 2017 [22]. In the measurements that we have conducted since, much has been learned with important implications for the possibility of a new kind of automated oxyfuel system [23, 24, 25, 26, 27].

The purpose of this two-part paper is to assemble these prior measurements together with recent measurements to draw some conclusions about the potential for ion currents as a technology for sensing in the oxyfuel cutting process, to establish the most important problems left to solve, and to present our early results for a fundamental electrical study of the oxyfuel flame. We consider five experimental configurations:

1. tests in a preheat configuration over temperature-controlled steel [22],
2. tests in a preheat configuration over temperature-controlled copper [25],
3. tests in a preheat configuration over plate steel [25],
4. tests while cutting steel [27],
5. measurements of the ion density inside the flame (part II).

We will discuss the first four configurations here, but the last topic is sufficiently complex that we will relegate it to a second part of this paper. The reader is presumed to be familiar with the oxyfuel cutting process.

In configurations 1-4, the torch was electrically connected to a precision power supply capable of operating in a constant-current or constant-voltage mode. Since standard welding hoses for oxygen and fuel gas service are electrically conductive, isolating the torch from the cutting machine required PTFE gas fittings and a Nomex sheet installed between the clamping blocks that support the torch. The work, table, and power supply were connected to earth ground. Voltages could be commanded in the range of ±12.5V and currents could be applied in the range $\pm25\mu$A. Voltages were measured over the same range, but currents could be measured as large as $\pm250\mu$A.

The is an Oxweld C-69 machine torch burning industrial grade (95% pure or better) methane. Preheat gas flow rates were measured using thermal mass flow meters and regulated with metering valves in a separate room from the experiment to eliminate thermal effects on the valves and regulators.

Figure 1 shows the experiment in configuration 1. Configuration 2 substituted a copper disc for the steel disc in configuration 1. Configurations 3 and 4 simply used un-cooled half-inch steel plates in various states of corrosion.

2 The Current-Voltage Characteristic

In every experiment conducted, regardless of the work piece material, and regardless of whether cutting oxygen was flowing, the relationship between voltage and current in the range of ±10V exhibited a consistent shape. Three distinct regimes naturally form in the shape shown in Figure 2. We already see here that components of the curve are quite consistent, but the flame's length and reactant mixture drastically influences the IV-characteristic.

We number the regimes 1 to 3 from left-to-right. We formally define regime 2 as the portion of the IV-characteristic over which the current magnitudes are sufficiently small that current changes linearly with voltage. By definition, regime 2 includes the non-zero voltage at which the flow of current is zero (called the floating potential). Regimes 1 and 3 are found when currents grow sufficiently (whether positive or negative) that saturation causes an abrupt deviation from the linear trend in regime 2.

Because currents in regime 2 are so small that no saturation has occurred, we call this the "Ohmic" regime. The availability of both positive and negative charge carriers is abundant here, so the electrical resistivity of the plasma limits the flow of current.

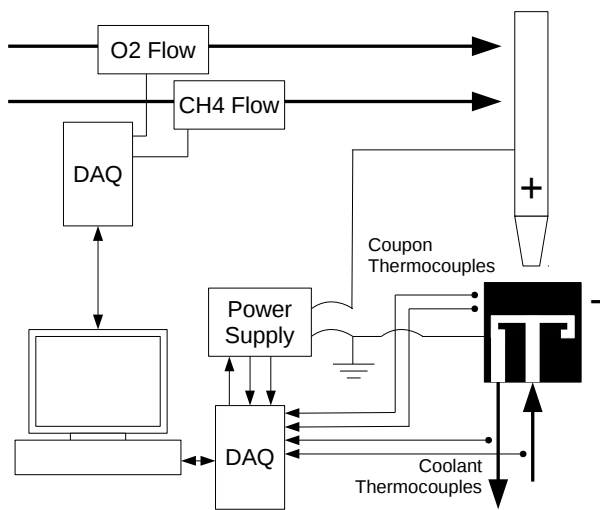It seems quite clear that regime 3 is saturation caused by a

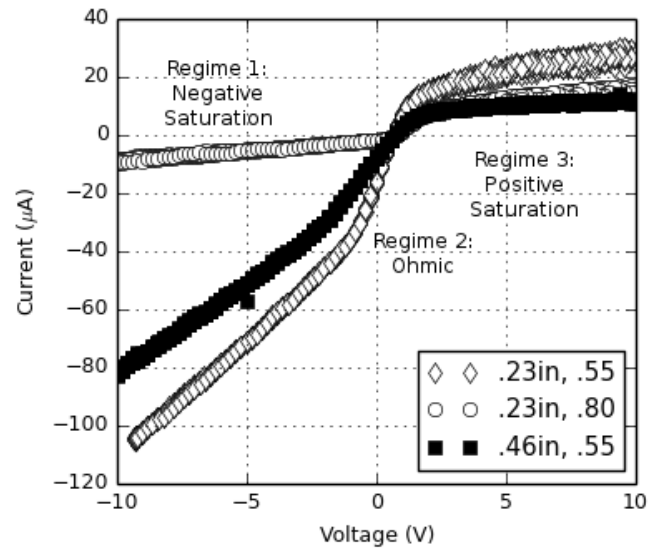**FIGURE 1**. The experimental configuration in test configuration 1.

FIGURE 2. Data collected over steel with different standoff distances and fuel/oxygen ratios.

saturation, the application of additional voltage does still cause additional current to flow, but at a reduced rate. Experiments in one-dimensional flames have demonstrated similar phenomena at similar voltages [28, 29, 30]. The explanation seems to be that when the flame is quite close to the tip, even the meager electrical mobility of H_3O^+ is sufficient to permit enhanced transport from the flame front. As we will address later, there is some direct evidence to substantiate this idea.

3 Standoff distance

The distance between the torch tip and the work piece is critical to maintaining cut quality, and since work pieces commonly warp, and since cutting tables rarely remain level for long, it is important to regulate the torch's offset from the work piece. Were a new sensing suite to displace the existing technologies, the measure of standoff distance is, perhaps, the first and most important test of its capabilities.

The original principles proposed by Mott et al. and even the patents since attempted to address this issue (and no others) by measuring inferring length of flame from tip to work by its electrical resistance [5]. This is made difficult by how severely the neighboring regimes can be distorted by adjusting the flame's operating condition (see Figure 2). For example, one might naively attempt to apply a constant voltage (or current) and measure the current (or voltage) to infer a total effective flame resistance, but this is complicated by the floating potential, which has been shown to vary significantly during a measurement [25]. Worse
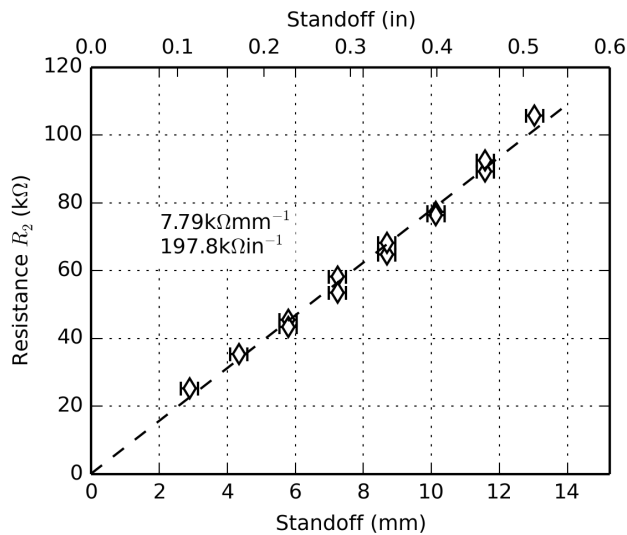
deficit of electrons in the vicinity of the work piece. When both electrons and positive ions are available in the region above the work piece, the net flow of charge from the surface will be the balance of the rate of impact of the two. As the torch is driven to positive voltage, electrons evacuate the region, the impact of negative charge declines, and the impact of positive charge either increases or is relatively unchanged. Either way, the net transfer of electrical charge is shifted in favor of positive impacts. This process can continue until electrons are completely evacuated from the region, and current is entirely due to the impact of positive ions; which are relatively unresponsive to these small voltages.

Regime 1, on the other hand, shows what we have previously called a "partial" saturation. While it may be presumed that a similar evacuation of negative charge carriers has caused

FIGURE 3. Ohmic-regime resistance versus the torch standoff distance.

FIGURE 4. Ohmic-regime resistance at three standoff distances versus the fuel/oxygen ratio.

still, this method would not detect error due to distortion from saturation.

3.1 Measurements made in configuration 1

We define the flame's resistance as the inverse of the slope of the IV-characteristic in regime 2. By definition, this is the electrical mode of operation where the electrons' finite mobility (electrical resistivity) limits the flow of current. The author's original paper in 2017 demonstrated the repeatable and reliable relationship between the regime 2 resistance, R_2, and the standoff distance shown in Figure 3.

These data were collected at a preheat gas flow rate of 9.4L/min (20scfh) and a fuel/oxygen ratio 0.55. The resistances were obtained by fitting piece-wise linear curves to the IV-characteristics.

Measurements taken while varying the fuel/oxygen ratio showed little change near the stoichiometric mixtures (0.5), but at richer mixtures more typical of cutting conditions, there is a trend towards higher resistances. Figure 4 shows the regime-2 resistances at three standoff distances while the fuel/oxygen ratio is varied (without varying total flow rate).

Near stoichiometric conditions, when the inner cone is so short that it nearly vanishes inside the torch tip, neither the flame location nor the regime 2 resistance is sensitive to fuel/oxygen ratio. However, at richer mixtures, precisely as the inner cone begins to elongate, there is a corresponding rise in the flame's apparent electrical resistance.

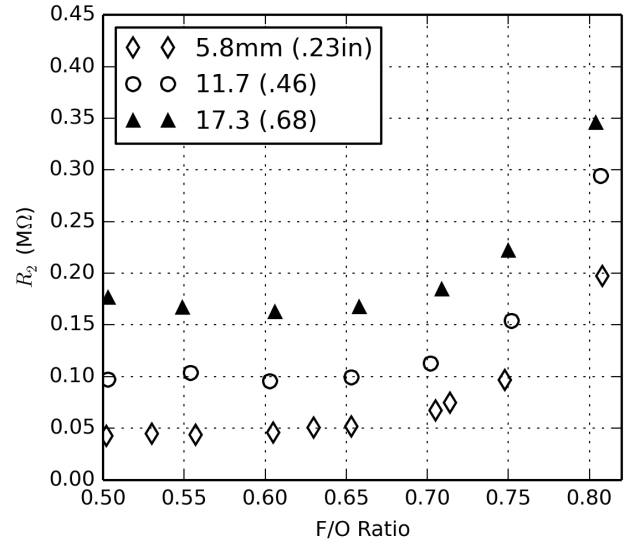Were this trend caused by an increase in electrical resistivity

everywhere in the flame, then the electrical resistance at the three heights would scale proportionally; a doubling of the resistance at small standoffs should correspond to a doubling of resistance at large standoffs. This is not what is observed; rather, it appears that the resistance at all heights has been equally augmented by the addition of some new series resistance that is equally observed at all heights.

From only these data, it seems that there is a region of high electrical resistance that grows upstream of the inner cone. That electrical resistance creates an offset, so that the slope of flame resistance versus standoff is preserved, but the curve no longer passes through the origin.

3.2 Measurements made in configuration 4

The same behaviors are readily observed while cutting, but with some important complications that may have been barriers to success for prior efforts. The oxyfuel cutting process is notoriously violent; with pulsating expulsions of molten iron and its oxides from the kerf. At the outset, it certainly seems safe to imagine that the flame's electrical characteristics will exhibit features that are equally complex. The method of fitting piece-wise curve fits is simultaneously difficult to apply in real-time and demonstrates undesirably poor performance in the presence of noise, so it is a practical necessity to identify a more robust approach.

We have already learned from preheat studies that the regime 1 currents can nearly vanish at rich fuel/oxygen ratios typical of cutting, the floating potential can be seen to vary unexpectedly
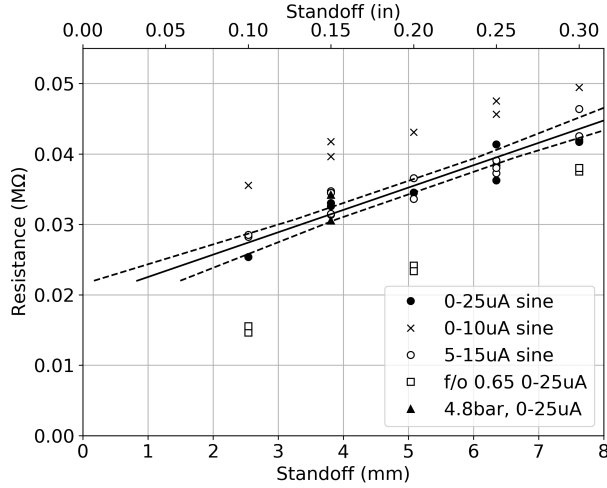
FIGURE 5. Regime 2 resistance measurements versus standoff distance while cutting 1/2-inch steel.
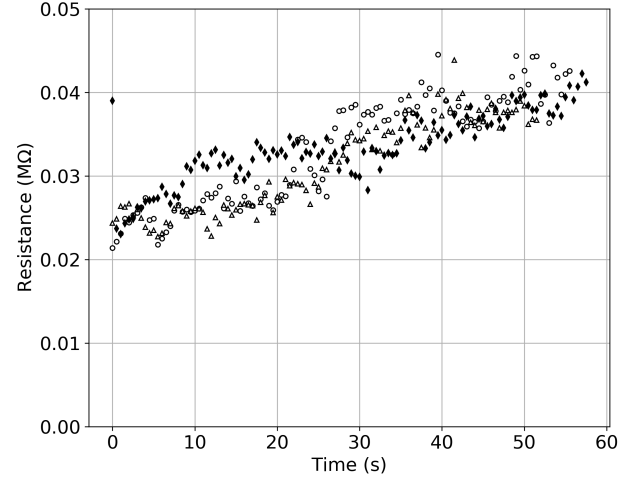

FIGURE 6. Regime 2 resistance while cutting plates on an incline. White circles and triangles were measured on the same plate. Black Diamonds were measured over a separate plate.

and significantly, and the range of voltages over which regime 2 can be found is seen to be alarmingly narrow. From these observations, we conclude that practical regime 2 resistance measurements require excitations of constant current and not constant voltage.

In a study published quite recently, 10Hz cosine current excitations with various offsets and amplitudes were forced between the torch and work piece while monitoring the resulting voltage [27]. By isolating only the signal content at 10Hz over an interval that need be no longer than portions of a second, the uncorrelated noise at other frequencies can be rejected just as is typically done in so-called "lock-in" amplifiers.

Figure 5 shows regime 2 resistance measurements collected using this method while cutting half-inch steel plate at constant speed, but while varying other conditions. The fuel/oxygen ratio was 0.78 and the total flow rate was 12L/min (26scfh). The cutting oxygen pressure was nominally 3.4bar (50psig), but for one series of tests it was increased to 4.8bar (70psig) with no effect on the measurements. To test the sensitivity to excitation, three current ranges are shown. To verify that the cutting process exhibits the same sensitivity to the gas mixture, a series of cuts were also performed at 0.65 fuel/oxygen ratio; the richest condition at which no sensitivity was noticed in preheat tests.

The results demonstrate that low-current, small amplitude signals must be avoided at rich conditions because they are corrupted by curvature in the extremely small regime 1 saturation we have already seen in Figure 2. Rich flames also exhibit the same offset observed in the preheat configuration, which vanishes at leaner conditions while preserving the slope.

A linear fit for standoff, s, through the cluster of data at the center is of the form

$$s(R_2) = mR_2 + b \qquad (1)$$
$$m = 315 \pm 48 \text{mm/M}\Omega$$
$$b = -6.1 \pm 1.7 \text{mm}$$

The dashed lines show upper and lower limits for the fit based on the covariance matrix for the coefficients. The most pessimistic estimates for the uncertainty of a standoff measurement based on the scatter observed might be $\pm$1mm ($\pm$0.04in). As we address in more detail in the original paper, some of this uncertainty is due to the limits of experimental control on standoff. We estimate the actual uncertainty to be nearer to $\pm$0.5mm ($\pm$.02in).

This argument is substantiated by similar resistance measurements taken while cutting plates with a deliberate incline from 2.5mm (0.10in) to 6.5mm (.25in) over a cut 300mm (12in) long. Figure 6 shows resistance measurements during three cuts; two on the same plate and the third on a fresh plate. The heights at the start and end of the torch motion were carefully measured before the cut. The scatter is roughly consistent to within $\pm$0.5mm while the largest deviations are slow arcs that re-converge at the beginning and end where the standoffs were carefully checked. Data from the same plate show the same curvature, while data from a different plate show new features. These deviations from a straight line appear to be a measurement of the plate's curvature during the cut.

Typical standoff distances are several mm (about 1/8in) or larger. Well trained manual operators can execute beautiful cuts with a torch cantilevered hundreds of mm (1ft or more) from their

hands. Over the course of a cut, were an operator to maintain a height better than ±1mm, variation of the torch angle by about 1/10 of a degree would be unacceptable. Meanwhile, we more than doubled the standoff in our tests with noticeable but tolerable impacts on the quality of cut. While this can hardly be said to be the final word on standoff confidence intervals, it is a starting point from which to suggest that ion current measurements may be more than adequate for the purpose.

4 Pierce success and loss-of-cut

Measurements in a preheat configuration showed that the flame resistance grew by 7.8kΩ per mm of standoff (Figure 3). During a cut, it only grew by about 2.8kΩ per mm (Figure 5). These divergent observations are repeatable and far too extreme to be explained by error. Why is this so? The answer yields methods for anticipating loss-of-cut and diagnosing a failed pierce operation using only regime 2 resistivity.

For a flame to exhibit reduced resistance with the addition of cutting oxygen while preserving all other parameters, we must accept that either the transport of ions in the flame is enhanced or there are more ions to transport. We might speculate that the presence of cutting oxygen would enhance turbulence and therefore transport, but we observed no change in resistance in Figure 5 when the cutting oxygen pressure was drastically increased.

Figure 7 shows the regime 2 resistance of four cuts with two standoff distances while varying the torch feed rate through a wide schedule of speeds with 50mm (2in) of cut at each speed. The lower standoffs are somewhat smaller than a typical cut, and show a repeatable trend toward slightly higher resistances at excessive speeds. The higher standoffs are significantly higher than a typical cut, and data show a severe rise in resistance as the cut is nearly lost due to the non-ideal conditions.

Regime 2 resistance measurements were performed while carrying out both successful and failed pierce operations. The signals were so divergent as to require no nuance in differentiating them. During a successful pierce operation, the detected currents were so large that the flame resistance appeared to be nearly zero. During a failed pierce operation, there were no detectable currents, so the flame resistance appeared infinite. The absence of current during a failed pierce persisted even as the torch was allowed to move over a cold plate with its cutting oxygen activated. The same was not true for edge starts; the torch needed to be over a plate for the current to be driven to zero.

There are two phenomena that, together, produce a self-consistent explanation for all of these observations.

1. The intense chemical reaction in the kerf contributes its own "secondary" ions to augment the "primary" ions in the preheat flame.
2. At excessive speeds or during failed pierce operations, some or all of the cutting oxygen washes over the face of the plate,
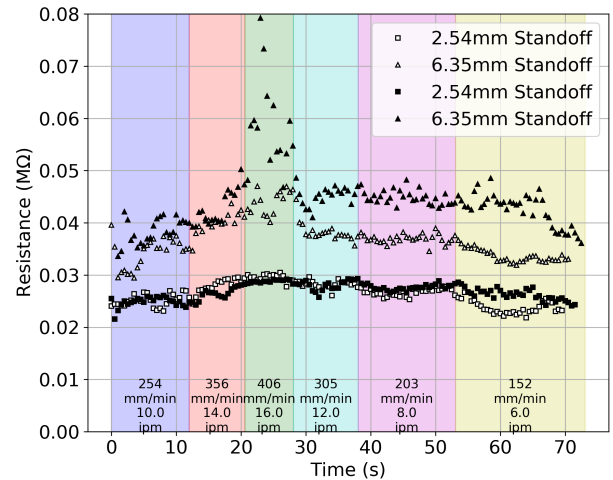

FIGURE 7. Regime 2 resistance during four cuts while maintaining standoff but varying feed rate.

forming an insulative layer between the flame and the plate.

The first of these is not entirely unexpected, but for the flame resistance to be divided by three, the quantity of ions must have roughly tripled. That indicates that despite the name we have given them, "secondary" ions can outnumber "primary" ions. In fact, during a pierce, when molten iron is deflected back into the preheat flame, the effect is so intense that primary ions are, apparently, negligible in quantity compared with secondary ions.

It may be surprising that the flow of oxygen could so effectively insulate the flame from a plate, but there can be no doubt about the cause. Tests without cutting oxygen over a plate and on the plate's edge show little to no change in regime 2 resistance, and tests while cutting show no measurable impact due to the cutting oxygen velocity. Furthermore, the noise in the regime 2 measurements is likely due to genuine oscillations in the ion concentrations with the natural pulsating expulsion of metal that can be observed in the kerf.

There is one disturbing piece of information here; regime 2 resistance can be strongly impacted by something other than the standoff distance. We argue that if the supervising controller is well designed, this is not especially troubling for the application of ion current sensing. These changes occur quickly and severely; far more so than could be explained by errors in plate level unless the work has spontaneously fallen from the table. In fact, these are reliable and repeatable diagnostics for severe problems in the cut health.

If a controller were to observe that the regime 2 resistance is inexplicably rising quickly and violently, what would the correct response be? We will establish later that more information can be gained by also scrutinizing the other regimes, but for now, we will operate on the assumption that no additional information is

available. There are two possible actions: (1) reduce the torch height, and (2) reduce the cutting speed to prevent loss-of-cut.

If we were to reduce the torch height due to an incorrect diagnosis of standoff change, collision would be most likely at small standoffs. Figure 7 demonstrates these effects are only slight at small standoffs, and it would not be a difficult matter to severely limit the rate or range of torch height changes to prevent violent motions. It would also be a simple matter for the controller to recommend temporary reductions in feed rate if regime 2 resistance measurements were to begin changing (up or down) faster than a certain rate.

Above all, if the resistance were seen to approach infinity, the controller could immediately raise a lost-cut alarm; an event unprecedented in the history of sensing in oxyfuel cutting systems.

5 Start and health of cut

So far, we have focused entirely on a single aspect of the IV-characteristic, and as we have already mentioned in the previous section, far more can be learned by scrutinizing its other aspects. If regime 3 is created by a saturation at the work surface, could measurements there be used to indicate ready-to-pierce or to verify the cut health measurements we discussed in the last section?

Early data collected in configuration 1 (over cooled steel) showed a trend between the temperature of the steel and the current levels in regime 3, but the results were never repeatable. In fact, during a single test lasting only 10 seconds, long after the temperature of the steel had been stabilized, the regime 3 current was observed to triple before slowly subsiding. Worse still; this behavior could not be reliably reproduced either.

5.1 Measurements in configurations 2 and 3

First, it is necessary to identify the cause of secondary ions. We have already established that they come from the work piece, but are they due to thermionic emission, to chemical action at the work surface, or to variations in the surface area that drastically changes when the metal melts?

Tests over cooled copper (configuration 2) allow experimental control of all these factors. Copper oxide is mechanically stable, so any initial chemical action will quickly subside in steady-state tests and the work surface will have a stable surface area. Moreover, thermionic emission from copper is sufficiently feeble in comparison with iron that it can be safely neglected. Meanwhile, when we perform an identical preheat operation over a cooled copper disc and an uncooled steel plate, the differences are striking.

Figure 8 shows the results of two tests over a copper disc over-plotted with a test over a steel plate. Tests over copper are so repeatable that it is not possible to distinguish the data points from one another. When the copper disc is varied in diameter
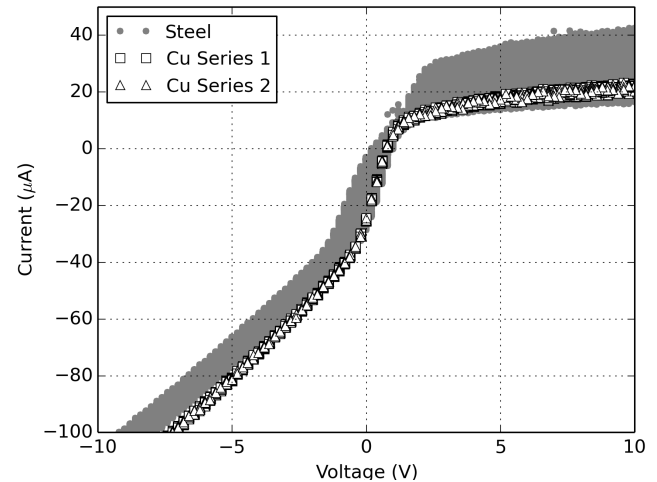

FIGURE 8. Tests over cooled copper discs and a test heating 1/2-inch steel plate

from 27 to 57mm (1.05 to 2.25in), when the surface of the copper is clean or rough, and when the disc is cold or glowing bright orange, these results do not change.

These facts withstanding, it seems that the regime 3 currents are due to chemical action at the work surface. To confirm, we repeated the same test over an iron plate that had been encrusted in salts by soaking the plate in a bleach-vinegar solution and allowing the solution to dry. The addition of salts are an old trick in the study of ion currents to artificially introduce additional ions. As we see in Figure 9, the effect is exaggerated in magnitude but identical in character to the effects we see over clean steel.

5.2 Ready-to-pierce tests in configuration 3

If regime 3 currents are enhanced by the chemical action at the work surface (or in the kerf), then there should be an obvious signature when the plate reaches its kindling temperature (auto-ignition temperature in an oxygen atmosphere). There should also be signatures for the reaction rate in the kerf while cutting.

In Figure 10, the regime 3 current was measured by applying +10VDC to the torch and applying a median value filter to the measured current. Four sections of 1/2-inch thick steel plate were fitted with thermocouples from underneath roughly 3mm (0.13in) from the top surface, and the known thermal load from the torch was used to estimate the material temperature at the work surface centered under the flame [25]. Two of the tests were conducted on plate with little corrosion that were wire-brushed clean, and two were performed on plate with heavy corrosion.

The results show that initial effects due to reaction with surface salts or flakes of corroded steel can cause bursts of regime 3 current, but as the bulk of the material heats, there is a consistent and repeatable rise in regime 3 current starting around
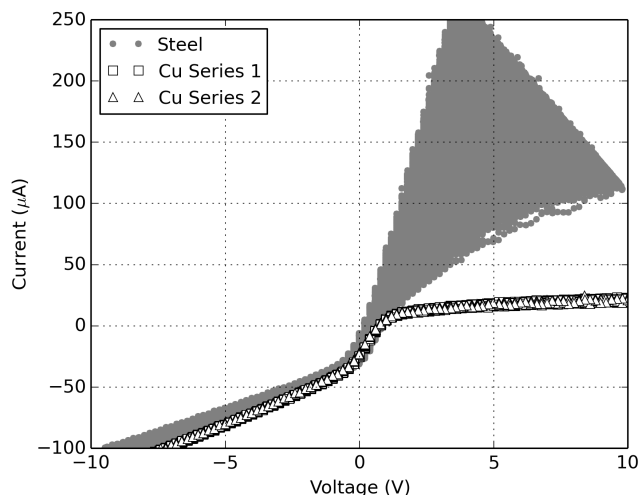
FIGURE 9. Tests over cooled copper discs and a test heating a 1/2-inch steel plate encrusted with salt
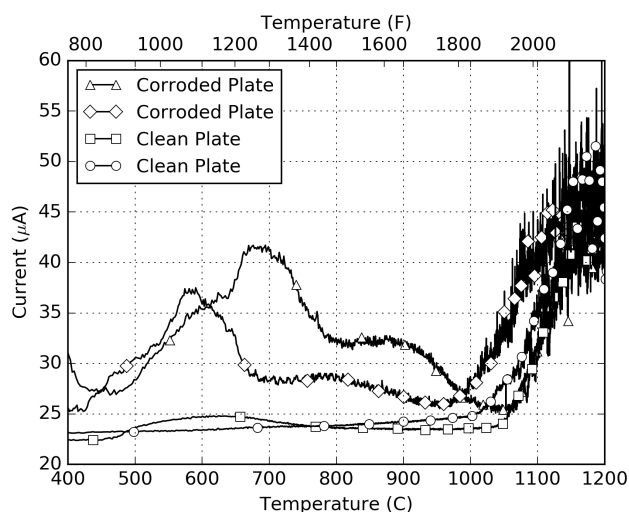

FIGURE 10. Current while holding the torch at 10VDC and preheating steel plates in various states of corrosion.

$1020 \pm 50°$C. This is consistent to measurements of steel's ignition temperature in an oxygen atmosphere [31, 32].

We propose using the regime 3 current as a ready-to-pierce criterion. In most oxyfuel cutting systems, torches are allowed to preheat the steel for a constant period before the cut is initiated. To avoid failed pierces, the dwell is often longer than strictly necessary. We propose to shorten the dwell to the minimum needed to ensure that any salts, oils, or corrosion have burned off, and then a ready-to-pierce signal can be generated simply by testing regime 3 current against a threshold.

We have already established that failed pierce operations are extremely easy to detect. If a process engineer wanted to be especially cautious, the cutting oxygen solenoid could be pulsed for a fraction of a second to allow a tiny puff of oxygen to flow. If the regime 3 current were to rise violently, the controller could proceed with the pierce operation in confidence. If the regime 3 current were to vanish momentarily, the preheat operation would need to be prolonged.

5.3 Cut health tests in configuration 4

If regime 3 current is an electrical signal indicating the rate of chemical action at the work, then it should also be able to serve as a means for monitoring the health of an active cut. Figure 11 shows IV characteristics taken while cutting a severely inclined plate at two feed rates. The first figure is a control test at a lower speed that successfully severed the plate. The second is a test at a slightly higher feed rate where the cut was lost as the standoff grew.

In both experiments, the IV characteristic prior to the successful pierce operation shows a familiar shape (see data at 20 seconds), but with a regime 3 current that is much larger than tests over copper. Once the cut was initiated, the regime 3 currents saturated the measurement, rising over 250μA (see data after 35 seconds). In the successful cut, the regime 3 current can be observed wagging intermittently so low as 150μA before recovering back above 250μA, and the regime 2 slope can be seen to decline with the increase in standoff. In the failed cut, the entire IV characteristic collapsed back to its preheat shape before slowly declining as the torch began to spill oxygen over cool non-reactive steel.

Regime 3 current is an indicator for cut health. Intermittent dips in regime 3 current are typical of even a healthy cut process, but prolonged signals below about 200μA were an indicator the cut was in jeopardy of being lost. In addition to monitoring standoff, a controller could intermittently check the regime 3 current to ensure that the signal is above a safe threshold. After repeated low measurements, the controller could recommend to the CNC that the feed rate be reduced to recover a healthy cut; just as an experienced operator might.

6 Fuel/oxygen ratio

Operators are universally instructed to adjust the fuel/oxygen ratio to torches by observing the inner cone length. These intensely luminous conical flame fronts are short and close to the torch tip under lean conditions, but as the fuel/oxygen ratio is increased, they elongate and form cones 3 to 5mm (0.1 to 0.2in) long. Books on the process recommend that torches be balanced so that their inner cones are as long as possible while still being stable. The same sources recommend maintaining standoff so that the inner cone tips just barely touch
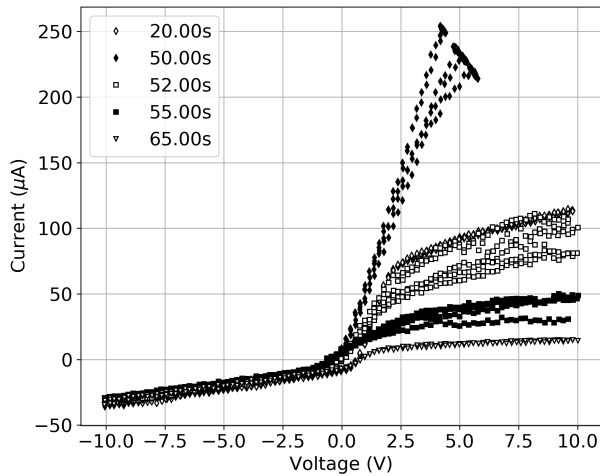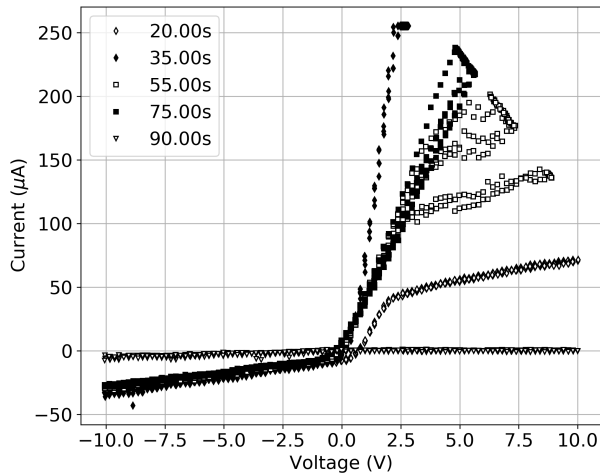
FIGURE 11. IV-characteristics during (top) a cut that succeeded and (bottom) a cut that was lost.

the work piece [33].

It is well understood that flame speeds are reduced when the fuel/oxygen ratio is changed far from stoichiometric conditions, so elongation of the inner cone is essentially a measure of the fuel/oxygen ratio [34]. It is also well understood that flame temperatures are maximum at rich conditions; especially for oxyfuel flames [35]. Can these visual observations be replicated with electrical measurements?

We have already commented in Sections 3 and 4 that the regime 2 resistance is sensitive to the cone length, which makes it only more desirable to devise a measurement to verify that the inner cones are stable.
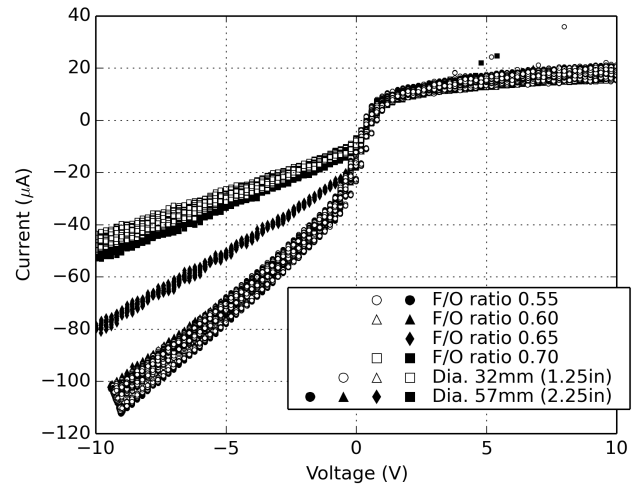

FIGURE 12. Tests over copper discs of different diameters while varying fuel/oxygen ratio.

6.1 Measurements made in configuration 2

Though we have not drawn attention to it yet, the figures we have already presented demonstrate remarkable changes in regime 1 as the fuel/oxygen ratio is changed. Figure 12 shows tests over copper discs with different diameters while maintaining the total flow rate and standoff, but while varying the fuel/oxygen ratio.

As we have seen already, regime 1 is quite stable and repeatable even while regime 3 is highly variable. When the torch is driven to negative voltages, the saturation occurs at the torch tip in the tiny region between the inner cone flame front and the tip. Figure 12 verifies that even before there are easily visible changes in the inner cone, there are electrical signatures indicating its motion.

We define the regime 1 saturation current as the current at which the piece-wise linear segments in regimes 1 and 2 intersect. This represents the magnitude of current necessary to evacuate electrons in the vicinity of the torch tip. While we could just as easily study the current at an arbitrary voltage somewhere safely in regime 1 like we did to study regime 3, the saturation current has the advantage of being utterly independent of standoff distance.

Figure 13 shows saturation currents measured by performing piece-wise linear fits of IV characteristics measured over steel at three standoff distances. At extremely large standoff distances, the slopes of both regime 2 and regime 3 flatten so severely, that it is very difficult to reliably identify the transition current with confidence near stoichiometric conditions.

It is not usually necessary to regularly monitor the fuel/oxygen ratio throughout cutting operations. It is more typical to occasionally check the preheat flames between operations
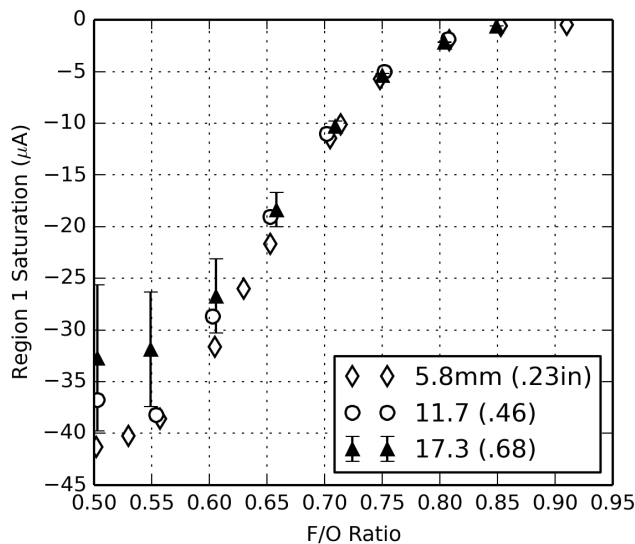
FIGURE 13.   Regime 1 saturation current plotted against fuel/oxygen ratio for three standoff distances.

to be certain they are still properly balanced. During a preheat operation, while the torch is positioned a known distance above a work piece, it would be a simple matter to test the regime 1 current to ensure it had not drifted. However, it would also be possible to perform a regime 1 slope measurement alongside the regime 2 slope measurements and calculate the intersection point. This could be done at any point in the cutting process.

7 Conclusions

Not only can the sensing typically performed in contemporary mechanized oxyfuel cutting systems can be replecated by ion current measurements, but so can parameters that even the most advanced systems do not measure. This includes

Standoff distance
Ready-to-pierce
Pierce success
Cut health monitoring
Fuel/oxygen ratio

These results motivate the idea of a mechanized system with no sensors, but a small electronic module tied to each torch. Digital communication or legacy analog and relay logic could be used to signal the CNC of each station's status. If our results so far can be replicated, such a system should out-perform any commercially available suite today.

It is clear that in the span of several years, much has been established about what is possible using ion currents. Still, there

are a number of important steps that still remain if these are to find wide adoption.

1. Standoff measurements should be repeated with a precise reference measurement to compensate for imperfections in the experimental control.
2. These studies should be expanded to include different torch tip geometries and fuel gases. These data are all using methane. While there is not reason to suspect that these conclusions are not extensible to other fuels, the work should be done.
3. Cut tests so far have only been on one thickness of plate, and the actual amplitudes of the regime 3 current are not known since the measurements were saturated. Are these amplitudes proportional to the rate of metal consumption as one might expect?
4. We have attributed unsteady regime 3 currents to the cyclic phenomena in the kerf. If this is so, it should be possible to correlate the signal with photography of events inside the kerf. These last two items together would add significant confidence in the cut health diagnostics.
5. We have made a number of assertions about where ions are located (or not located) in the flame, but spatially resolved measurements should be conducted to verify these claims.
6. A statistically significant number of pierce operations should be conducted using the criteria recommended in Section 5. Is the method reliable?

We begin to deal with item 5 in part II of this paper.

REFERENCES

[1] Calcote, H. F., 1957. "Mechanisms for formation of ions in flames". *Combustion and Flame,* **1**(4), pp. 385–403.
[2] Calcote, H. F., 1961. "Ion production and recombination in flames". In Eighth Symposium on Combustion, Vol. 8, Combustion Institute, pp. 184–199.
[3] Knewstubb, P. F., and Sugden, T. M., 1958. "Mass spectrometry of the ions present in hydrocarbon flames". In Seventh Symposium on Combustion, Vol. 7, Combustion Institute, pp. 247–253.
[4] Fialkov, A. B., 1997. "Investigations on ions in flames". *Progress in Energy and Combustion Science,* **23**, pp. 399–528.
[5] Mott, C., Chouinard, A., and Harding, R., 1944. Torch

device. US Patent 2364645, December. National Cylinder Gas Co. 266/23.

[6] Boucher, P. E., 1928. "The drop of potential at the cathode in flames". *Physical Review, 31*, May.

[7] Banta, H., 1929. "The mobility of positive ions in flames". *Physical Review, 33*, February.

[8] Anderson, N., 1960. Method and apparatus for automatic torch positioning. US Patent 2949391. Air Reduction Co. 148/9.

[9] Brouwer, F., 1966. Height control transducer. US Patent 3290032, December. Stewart Warner Corp 266/23.

[10] Stolin, B., and Brown, R., 1974. Torch height control for flame cutting machines. US Patent 3823928, July. Caterpillar Tractor Co. 266/23 M.

[11] Richardson, R., 1982. Torch height sensing apparatus. US Patent 4328049, May. Caterpillar Tractor Co. 148/9 R.

[12] Martin, C., 2018. Work piece condition detection using flame electrical characteristics in oxyfuel thermal processing equipment. US Patent 10067496 B2, September.

[13] Chorpening, B. T., Thornton, J. D., Huckaby, E. D., and Benson, K. J., 2007. "Combustion oscillation monitoring using flame ionization in a turbulent premixed combustor". In Proceedings of the ASME, Vol. 129, pp. 352–357.

[14] Li, F., Xu, L., Du, M., Yang, L., and Cao, Z., 2017. "Ion current sensing-based lean blowout detection for a pulse combustor". *Combustion and Flame, 176*, pp. 263–271.

[15] Henein, N., Bryzik, W., Abdel-Rehim, A., and Gupta, A., 2010. "Characteristics of ion current signals in compression ignition and spark ignition engines". *SAE International Journal of Engines, 3*(1), April, pp. 260–281.

[16] Badawy, T., Shrestha, A., and Henein, N., 2012. "Detection of combustion resonance using an ion current sensor in diesel engines". *ASME Journal of Engineering for Gas Turbines and Power, 134*, pp. 052802–1–9.

[17] Rao, R., and Honnery, D., 2015. "A simplified mechanism for the prediction of the ion current during methane oxidation in engine-like conditions". *Combustion and Flame, 162*, pp. 2928 – 2936.

[18] Rao, R., and Honnery, D., 2017. "A study of the relationship between NOx and the ion current in a direct-injection diesel engine". *Combustion and Flame, 176*, pp. 309–317.

[19] Jones, A., 1988. "Flame failure detection and modern boilers". *Journal of Physics E: Scientific Instruments, 21*, pp. 921–928.

[20] Mierzwinski, E. P., 1991. "Integrated furnace control". *IEEE Transactions on Industry Applications, 27*(2), pp. 257–261.

[21] Weinberg, F., Dunn-Rankin, D., Carleton, F., Karnani, S., Markides, C., and Zhai, M., 2013. "Electrical aspects of flame quenching". In Proceedings of the Combustion Institute, Vol. 34, pp. 3295–3301. doi:10.1016/j.proci.2012.07.007.

[22] Martin, C., Leonard, C., and VonFricken, J., 2017. "A study of the electrical characteristics of an oxy-fuel flame". *Experimental Thermal and Fluid Science, 88*, pp. 65–72.

[23] Martin, C., 2017. "Mechanized oxyfuel control using ion current sensing". *The Welding Journal, 96*(5), May, pp. 154–162.

[24] Martin, C., 2017. "Replacing mechanized oxyfuel cutting sensors with ion current sensing". In Proceedings of the ASME 2017 Manufacturing Science and Engineering Conference, pp. MSEC2017–2789.

[25] Martin, C. R., 2018. "A study of ion currents in an oxyfuel flame due to work surface chemical action". *Experimental Thermal and Fluid Science, 98*, pp. 239–250.

[26] Martin, C., 2018. "Electrical signatures for chemical action at the work surface in an oxyfuel flame". In Proceedings of the ASME 2018 Manufacturing Science and Engineering Conference, pp. MSEC2018–6354.

[27] Pond, T. L., and Martin, C. R., 2019. "Electrical characteristics of the oxyfuel flame while cutting steel". *Experimental Thermal and Fluid Science*, May. Accepted.

[28] Speelman, N., Kiefer, M., Markus, D., Maas, U., de Goey, L., and van Oijen, J., 2015. "Validation of a novel numerical model for the electrical currents in burner-stabilized methane-air flames". In Proceedings of the Combustion Institute, Vol. 35, pp. 847–854.

[29] Speelman, N., de Goey, L., and van Oijen, J., 2015. "Development of a numerical model for the electric current in burner-stabilised methane-air flames". *Combustion Theory and Modeling, 19*(2), pp. 159–187.

[30] Xiong, Y., Park, D. G., Jik, L. B., Ho, C. S., and Suk, C. M., 2016. "Dc field response of one-dimensional flames using an ionized layer model". *Combustion and Flame, 163*, pp. 317–325.

[31] Bolobov, V. I., 2001. "Conditions for the ignition of iron and carbon steel in oxygen". *Combustion, Explosion, and Shock Waves, 37*(3), pp. 292–296.

[32] Osawa, N., Sawamura, J., Ikegami, Y., and Okamoto, N., 2012. "Study of heat transfer during piercing process of oxyfuel gas cutting". *Welding in the World, 56*(3-4), pp. 2–10.

[33] The Linde Air Products Company, 1961. *The oxy-acetylene handbook*. Union Carbide Corp.

[34] Payman, W., 1923. "The propagation of flame in complex gaseous mixtures. part v. the interpretation of the law of speeds". *J. Chem. Soc., Trans., 123*, pp. 412–420.

[35] Glumac, N. G., 2007. "Flame temperature predictions and comparison with experiment in high flow rate, fuel-rich acetylene/oxygen flames". *Combustion Science and Technology, 122*, pp. 1–6.